ACS APPLIED MATERIALS & INTERFACES

www.acsami.org

Research Article

A Physically Triggered Cell Death via Transbarrier Cold Atmospheric Plasma Cancer Treatment

Dayun Yan,[‖,*] Qihui Wang,[‖] Manish Adhikari,[‖] Alisa Malyavko, Li Lin, Denis B. Zolotukhin, Xiaoliang Yao, Megan Kirschner, Jonathan H. Sherman, and Michael Keidar*

Cite This: https://dx.doi.org/10.1021/acsami.0c06500

Read Online

ACCESS | Metrics & More | Article Recommendations | Supporting Information

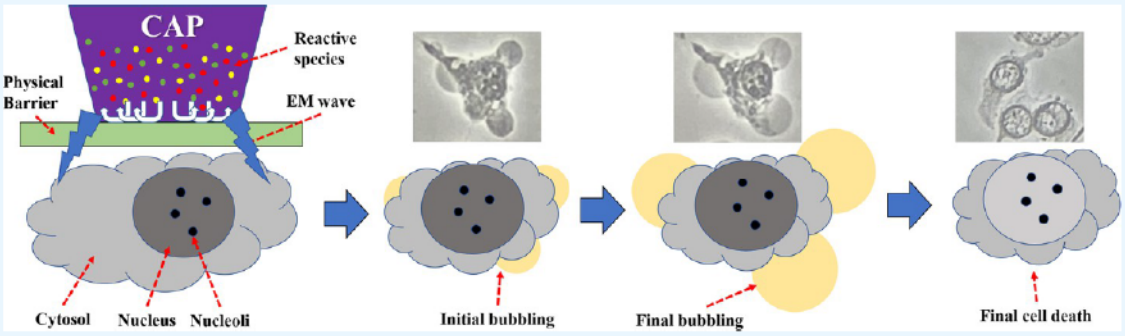

ABSTRACT: Cold atmospheric plasma (CAP) is a near room-temperature ionized gas composed of highly reactive species. CAP also generates thermal radiation, ultraviolet radiation, and electromagnetic (EM) waves. So far, nearly all biological effects of CAP have relied on the chemical factors in CAP. Here, we first show that the EM emission from CAP can lead to the death of melanoma cells via a transbarrier contactless method. Compared with reactive species, the effect of the physical factors causes much stronger growth inhibition on a reactive species-resistant melanoma cell line B16F10. Such a physically triggered growth inhibition is due to a new cell death type, characterized by the rapid leakage of bulk solutions from the cells, resulting in cytoplasm shrinkage and bubbling on the cell membrane. The physically based CAP-triggered cell death can occur even there is a macroscale gap between the bulk CAP and cells, which includes an air gap (~8 mm) and a dielectric material of the dish or plate (~1 mm). Either a too large or a too small gap will inhibit such cell death. The physically triggered cellular pressure may cause the bubbling on cells, which can be inhibited in a hypotonic environment via the extracellular osmotic pressure. This study builds a foundation to use CAP as a physically based noninvasive cancer treatment.

KEYWORDS: *cold atmospheric plasma, electromagnetic wave, cell death, melanoma, noninvasive cancer treatment*

INTRODUCTION

Skin cancer is one of the most common global malignancies. This broad category can be divided into melanoma and nonmelanoma skin cancer. Although nonmelanoma cancers such as basal cell carcinomas and squamous cell carcinomas are more common in the population, melanoma is the deadliest category of skin cancers.[1−3] Currently, there is a variety of different treatment options for melanoma. However, there is a constant need for more effective and noninvasive therapies, which do not require the medical instruments into the body to perform the therapy.[4−6]

Cold atmospheric plasma (CAP) is a near room-temperature ionized gas achieved in a nonequilibrium discharge at atmospheric pressure in the air mixed with inert gases such as helium and argon.[7,8] CAP is composed of nonequilibrium ionized particles, including neutral particles, ions, and electrons as well as highly reactive species and other chemical factors. The reactive species impact a variety of cells such as bacterial, plant, and mammalian cells in a multitude of ways.[9,10] However, a direct interaction of reactive species and cells is necessary for the biological and chemical effects of CAP *in vitro*. The conventional method of using CAP as a reactive species source limits its range of applications.

The conventional chemical CAP treatment leads to apoptosis of mammalian cells, a natural cellular response to an increase in reactive species intracellularly. CAP-triggered apoptosis follows a typical apoptotic pathway with changes in cell morphology including cell shrinkage, DNA fragmentation, membrane budding, and formation of the final apoptotic body

Received: April 14, 2020
Accepted: July 10, 2020
Published: July 10, 2020

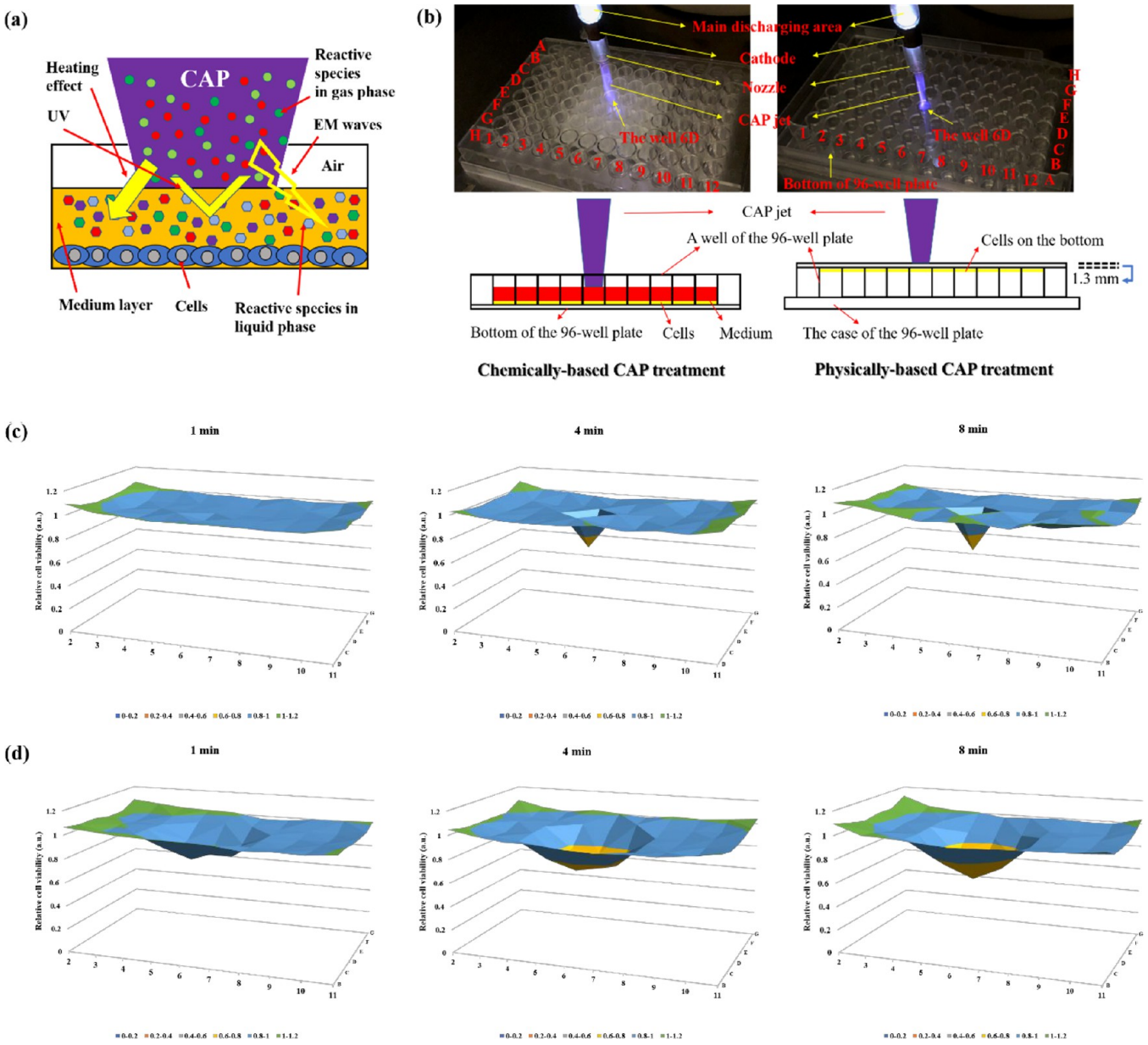

Figure 1. Chemically based CAP treatment and the physically based CAP treatment. (a) Chemical and physical factors in the CAP treatment. (b) Chemical treatment and physical treatment. Here, as an example, the physical CAP treatment was performed by treating the bottom of an inverted 96-well plate. The treated well was the well 6D on a 96-well plate. The gap between the CAP nozzle and the bottom of the 96-well plate was 25 mm. (c) 2D cell viability maps of the chemically based CAP treatment on a 96-well plate. (d) 2D cell viability maps of the physically based CAP treatment on a 96-well plate. All experimental conditions were the same in two different treatment strategies. The data are presented as the mean of four independent experiments. The original data are shown in Figure S3.

with membranous vesicles.[11,12] Although some groups have found markers of necrosis based on flow cytometry data, the corresponding mechanism is not clear or well understood, making it difficult to definitively conclude necrotic cell death.[13−16]

Aside from chemical factors, CAP produces three physical factors including thermal radiation, ultraviolet (UV) radiation, and electromagnetic (EM) waves in the range of 10−100 GHz.[17,18] Until now, all these physical factors have been thought to have negligible roles in cancer cell function and death following CAP treatment due to a lack of direct evidence of cellular responses to these factors.[19,20] However, the physical factors may be responsible or play important roles in the anticancer effect in CAP treatment both *in vivo* and *in vitro*.

In this study, we show the experimental evidence of a strong anticancer effect on B16F10 melanoma cells *in vitro* caused by electromagnetic emission from CAP. We initially demonstrate that CAP treatment can cause a great amount of cell death through an indirect, contactless method across a physical barrier (>1 mm). When cell viability is compared after conventional chemical treatment and this novel physical treatment, physical treatment achieves a more significant reduction in cell viability. A new type of cell death has also been noted in cells after physical CAP treatment, which could be contributing to the physically triggered anticancer effect. This cell death is characterized by rapid leakage of bulk water

https://dx.doi.org/10.1021/acsami.0c06500
ACS Appl. Mater. Interfaces XXXX, XXX, XXX−XXX

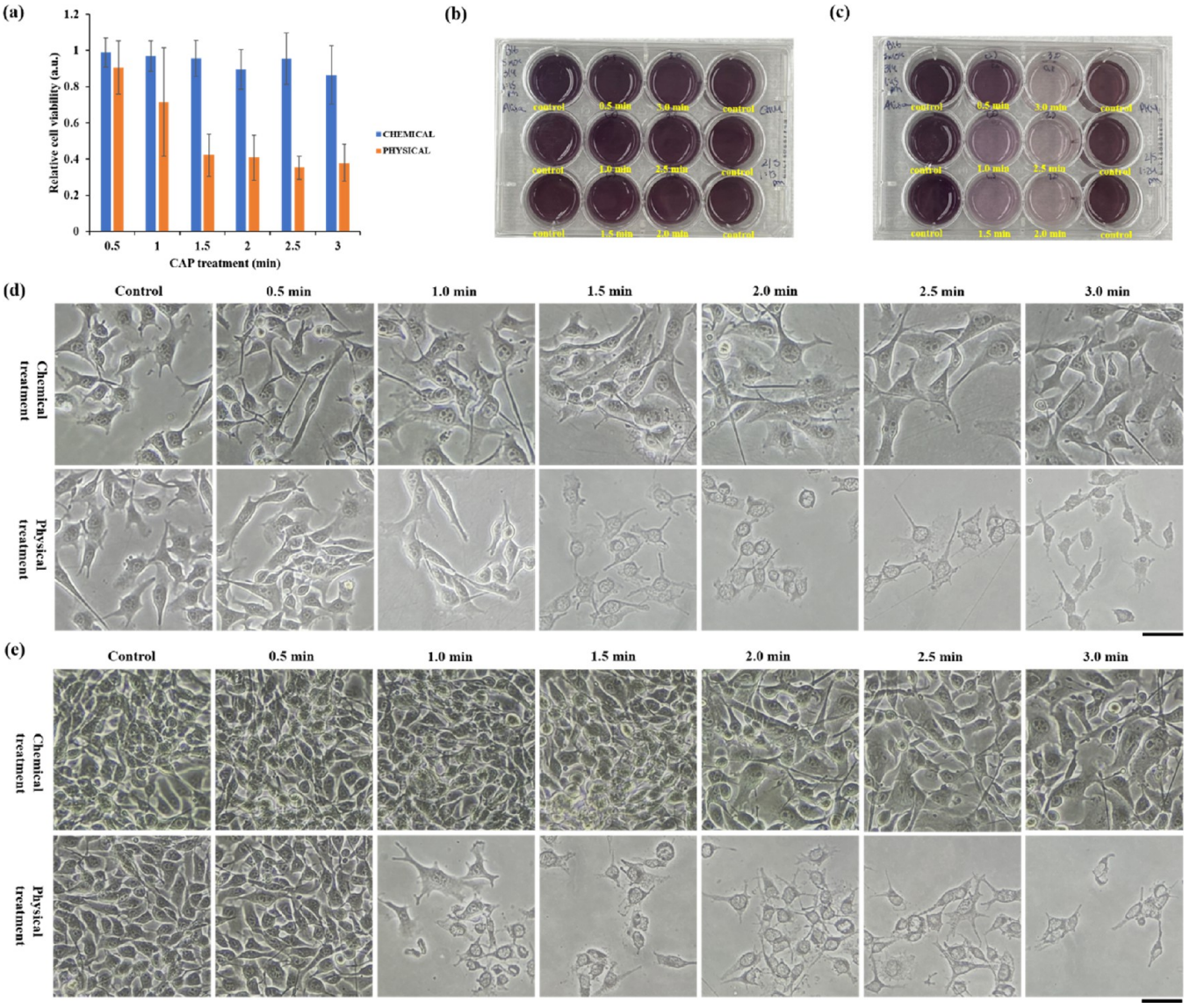

Figure 2. Drastically different cellular responses to the chemically and physically based CAP treatments. (a) Chemical and physical inhibitions of the cell viability. The data are presented as the mean of six independent experiments. (b) MTT assay on a 12-well plate after the chemically based treatment. (c) MTT assay on a 12-well plate after the physically based treatment. Some treatment information was shown on the cases of two photos here, including the treatment time in the specific well. The data processing of the cell viability assay is illustrated in Methods and Materials. (d) Microscopic images of the cells 1 day after the treatment (0.5−3 min). (e) Microscopic images of the cells 2 days after the treatment (0.5 min−3 min). The scale bar is 50 μm (black). For the chemical treatment, the gap between the nozzle and the cells was 37 mm. For the physical treatment, the gap between the nozzle and the bottom surface was 19 mm. The flow rate was 1.53 lpm. The microscopic imaging was performed using a Nikon TS100 inverted phase-contrast microscope.

from the cytoplasmic membrane, which results in visible bubbling on the cellular surface. The bubbling mechanism has been investigated through exerting osmotic pressure using hypotonic solutions. This study builds the foundation to understand the roles of physical factors of CAP in cancer cell death. With this knowledge, a more complete mechanism of CAP can be proposed, which will allow for greater translational use of CAP as a physically based noninvasive anticancer therapy.

RESULTS

Effects of Chemical and Physical CAP Treatments. Conventionally, *in vitro* CAP treatment is performed by treating cells cultured in dishes or multiwell plates where the plasma directly interacts with the medium covering the cells (Figure 1a). This strategy is an effective way to study the effect of reactive species on mammalian cells, particularly the cancer cells in this case. However, this strategy may interfere with or even completely block the physical effect of CAP on cells due to the bulk aqueous environment. Conventional CAP treatment also results in both the chemical and physical factors affecting the cell, making it difficult to unravel the effect of each factor and obtain a clear understanding of the underlying mechanism. To observe the purely physical effect of CAP, we used a novel technique to completely preclude all chemical factors. Throughout the study, physical CAP treatment was performed by inverting multiwell plates such as 96-well and 12-well plates and treating from the back, as shown in Figure 1b. The same protocol was done for various dish sizes ranging from 100 to 35 mm dishes. The detailed description of the

https://dx.doi.org/10.1021/acsami.0c06500
ACS Appl. Mater. Interfaces XXXX, XXX, XXX−XXX

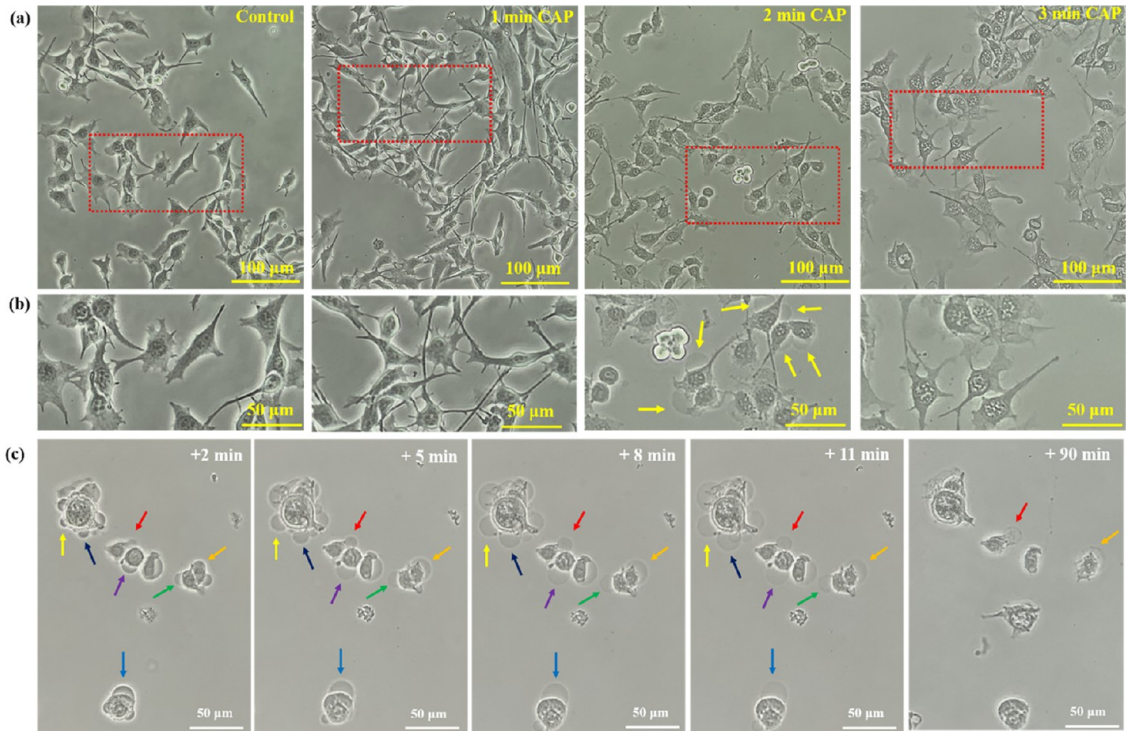

Figure 3. Quick morphological change of B16F10 cells immediately after the physically based CAP treatment. (a) Imaging with a low magnification. (b) Zoomed-in images for the red dotted boxes in panel (a). The yellow arrows mark the bubbles on the cellular membranes. B16F10 cells were seeded with a density of 1×10^5 cells/mL on a 35 mm glass-bottom dish and cultured for 1 day before the treatment. After the treatment, 1.5 mL of medium was added in the 35 mm glass-bottom dish immediately (<30 s). The images were taken 8 min after the treatment. (c) Growth of single bubbles after 2 min of CAP treatment. For all cases, the gap between the nozzle and the bottom surface was 27 mm. The flow rate was 1.53 lpm. The arrows mark the growth of seven specific bubbles on the cellular membrane. "+ *x* min" means that the photo was taken at *x* min after the CAP treatment. In the rightmost photo, the disappearance of certain cells and the appearance of new cells could be due to the detachment and the migration of cells, respectively. The images were taken using a Nikon TS100 inverted phase-contrast microscope.

protocols for both chemical and physical CAP treatments is stated in Methods and Materials. Physical CAP treatment causes 2D growth inhibition, which is showed on treated 96-well plates using 2D cell viability maps. The protocol to generate 2D cell viability maps is illustrated in Figure S1. In addition, we demonstrate that simply keeping the plates in an inverted position will not cause growth inhibition of B16F10 cells (Figure S2).

The conventional efficacy of chemical CAP treatment is determined by the reactive species. Therefore, if a cell line is resistant to reactive oxygen species (ROS) or reactive nitrogen species (RNS), it will also be resistant to chemical CAP treatment. B16F10 melanoma cells are very resistant to reactive species, particularly ROS such as H_2O_2.[21] We initially compared the amount of growth inhibition seen following chemical CAP treatment versus physical CAP treatment. Compared to chemical CAP treatment, physical CAP treatment not only has a greater impact on growth inhibition but is also able to impact a wider area (Figure 1c,d). Chemical CAP treatment only causes growth inhibition in the treated well, 6D, whereas physical CAP treatment noticeably inhibits the growth of melanoma cells in at least eight wells surrounding the treated well 6D.

The CAP treatment on a 12-well plate shows a similar but more drastic difference between chemical CAP and physical CAP treatments. Protocols are illustrated in Methods and Materials. It is found that 3 min of chemical CAP treatment causes very minimal growth inhibition of B16F10 cells. On the other hand, just 1.5 min of physical CAP treatment resulted in nearly 60% growth inhibition of B16F10 cells (Figure 2a–c). The increased growth inhibition following physical CAP treatment is thought to be a result of a new type of cell death. Microscopic imaging was performed at 1 day and 2 days of post-treatment, and novel changes were seen in these physically CAP-treated cells (Figure 2d,e). These cell changes can be characterized by aggregation of the cytoplasm toward the nucleus and the nucleus becoming colorless, which can signify a loss of nuclear components. We noted that these changes remained for several days following the treatment. We did not witness any cell duplication, cell movement, or cell to cell interaction, leading us to believe that these cells were in a somewhat "fixed" state. We conclude that these new cellular changes are evidence of a new type of cell death, which is independent of chemical CAP factors and is the reason for physical CAP treatment, leading to such strong growth inhibition on a reactive species-resistant cell line B16F10. Similar physically based growth inhibition was also observed in several other cancer cell lines (data not shown here).

Bubbling Is an Early Feature of the Novel Cell Death. Apoptosis is the main mechanism of cell death seen in nearly all *in vitro* studies; however, we have observed a new type of cell death with novel corresponding cellular changes. To further investigate the transition from a normal cellular shape to the observed fixed cellular shape, we started by observing the immediate morphological changes of B16F10 cells after physical CAP treatment. We did not do in situ observation during the CAP treatment. However, we did observe the changes occurring in B16F10 cells immediately after CAP

https://dx.doi.org/10.1021/acsami.0c06500
ACS Appl. Mater. Interfaces XXXX, XXX, XXX−XXX

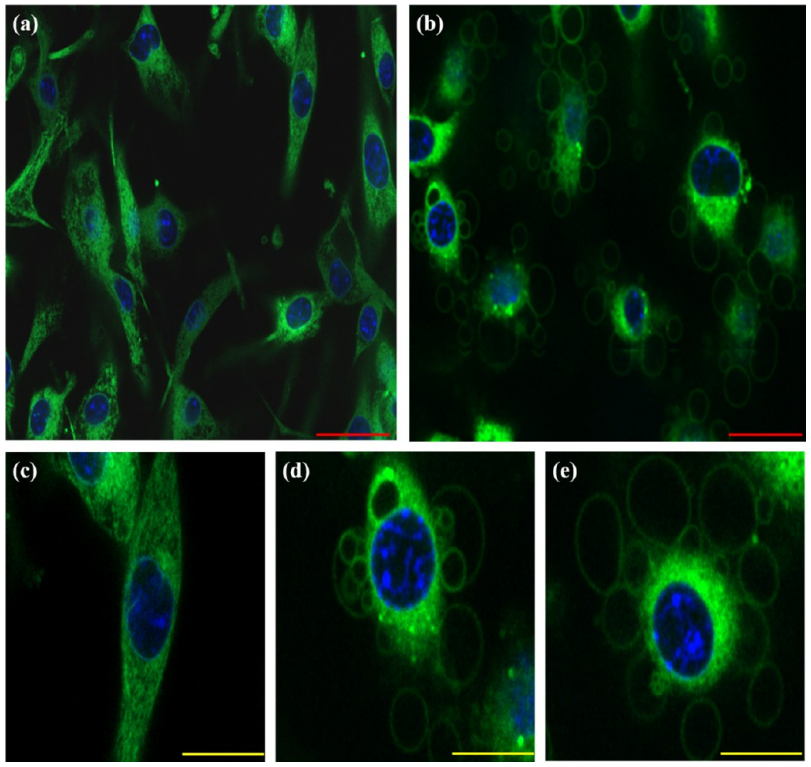

Figure 4. Live fluorescence imaging for the cellular change at 20 min after the physically based CAP treatment. (a) Control before the treatment. (b) Twenty minutes after the treatment. (c) Zoomed-in photo of the control. (d) Example of the bubbling on a single cell. The growth of the small bubbles is illustrated in Video S1. (e) Another example of the bubbling on a single cell. The microtubules and DNA (nucleus) are shown in green and blue, respectively. The scale bars are 40 μm (red) and 20 μm (yellow). All images were processed using ImageJ software.

treatment lengths of 1, 2, and 3 min. As shown in Figure 3a, a noticeable change in cell morphology is initially noted after a CAP treatment of 2 min. A significant shrinkage of the cytoplasm and a change in the nucleus can be observed. Several bubbles can be seen forming on the cellular membrane of CAP-treated cells as well, some of which are as large as the cell they are originating from. When the CAP treatment extends to 3 min, the bubbles disappear and the nucleus adapts a checkerboard color pattern, similar to the fixed cells shown in Figure 2d,e. At this time point, the nucleus is observed to have more white areas compared to observations made at shorter treatment time points. Additionally, the black dots, which could be the nucleoli, become more apparent in treated cells due to the whitening of the nuclei compared to cells in the control group. The size of the nucleus does not show any noticeable change. This cell morphology is a typical feature of physically treated cells immediately after treatment, which directly explains the fixed cell features observed 1 and 2 days after CAP treatment (Figure 2d,e).

The bubbling on the cell membrane is the most noticeable feature of the physical effect on B16F10 cells. Typical bubbling seen in B16F10 cells is presented in Figure S4. We performed a continuous observation of the bubbling over a while after physical CAP treatment. To observe clear bubble growth on a single cell, the seeding cell density should be relatively low (4×10^4 cells/mL). The cells were seeded in 35 mm glass-bottom dishes and cultured for 1 day before treatment. The growth of a bubble typically takes 8−11 min after CAP treatment (Figure 3b). As the bubbles grow larger, the inner composition of the bubbles becomes lighter and more transparent. This could suggest a slow dilution of the internal components as the bubble expands. No further morphological change is seen in the shrunken cells, other than what has been described previously, during this process or at the time when the bubbles reach their maximum sizes. Therefore, bubbling appears to be a process that occurs after the aggregation of the cytoplasm. The bubbles disappear from the membrane either by detachment or another mechanism approximately 90 min after CAP treatment. In Figure 3b, the debris of two bubbles can be seen remaining on two cells at 90 min after the treatment. As shown in Figure S5, we also observed the long evolution (31 min) of the CAP-treated B16F10 cells with a higher density (1×10^5 cells/mL). There is no further morphological change of the shrunken cells during the whole observation period. Many small, detached bubbles also are found in the extracellular space in Figure S5, which is the evidence supporting the detachment mechanism of the bubbles.

The phase-contrast imaging solely provides evidence of the morphological changes of cells. To investigate changes occurring at the cellular chemistry level, we performed live-cell fluorescence imaging. The detailed protocol is listed in Methods and Materials. Microtubules and DNA were stained using BioTracker 488 Green microtubule cytoskeleton dye (Sigma-Aldrich) and Hoechst 33342 (Thermo Fisher Scientific), respectively. The stained B16F10 cells were incubated for 15 min inside the CO_2 incubator. Then, the B16F10 underwent 4 min of physical CAP treatment, centered on the bottom of the dish. The gap between the nozzle and the bottom surface was 27 mm, and the flow rate was 1.53 lpm. After treatment, the dish was immediately placed upright and replenished with fresh RPMI-1640 media for confocal imaging. The staining was visualized and imaged using a Carl Zeiss 710

https://dx.doi.org/10.1021/acsami.0c06500
ACS Appl. Mater. Interfaces XXXX, XXX, XXX−XXX

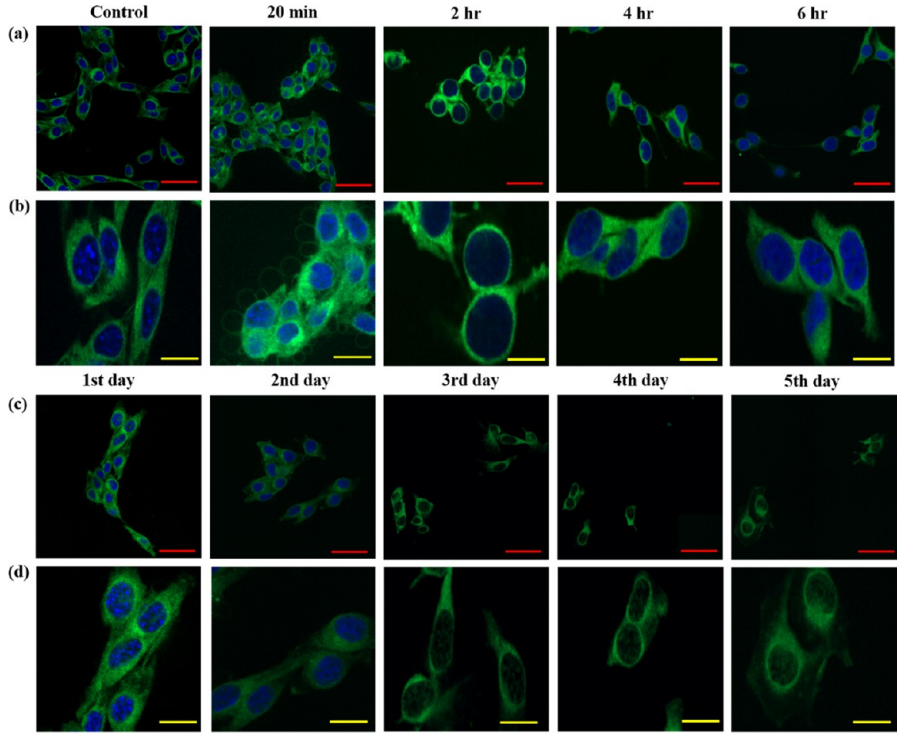

Figure 5. Fluorescence imaging of the physically based CAP-treated B16F10 cells over a long timescale. (a) Control before the treatment and the treated cells were observed 20 min, 2 h, 4 h, and 6 h after the treatment. (b) Zoomed-in photos. (c) CAP-treated cells were observed 1, 2, 3, 4, and 5 days after the treatment. (d) Zoomed-in photos. The microtubules and DNA (nucleus) are shown in green and blue, respectively. The gap between the nozzle and the bottom surface was 27 mm. The flow rate was 1.53 lpm. The scale bars are 40 μm (red) and 20 μm (yellow). All images were processed using ImageJ software.

spectral confocal microscope. Due to the operation of the imaging process, the first image was captured at 20 min after CAP treatment. Therefore, we were unable to capture the immediate changes occurring in the cells before the 20 min time mark. However, as we demonstrated above, the basic features of bubbling and the cytosol shrinkage will not change since the eighth min after the treatment.

The live fluorescence imaging confirms that the initial feature of the novel cell death is characterized by the formation of bubbles on the cellular membrane (Figure 4a,b). The light green surface of the bubbles is most likely due to the reflection of green fluorescence on the interface of the bubbles. The lack of fluorescence within the bubbles suggests that there may be an absence of organelles in the bubbles (Figure 4d,e). Thus, we propose that the bubbling is due to the leakage of water or cellular solution outside the cell membrane. The bubbles range in size from being as large at the nucleus to being as large as the entire cell itself (Figure 4d,e). A "grape-like" aggregation of bubbles can be seen in Figure 4d,e. It is believed that this aggregation pattern is due to the formation of new, smaller bubbles near or within the already formed larger bubbles. We also captured the dynamics of bubble growth on the cell membrane (Videos S1 and S2). In these two videos, the formation of new bubbles initiates from a single site on the cell membrane, potentially where a membrane pore or channel is present. Another clear feature is the change in the cytoskeletal structure. Filamentous microtubules are observed throughout the control cell (Figure 4c), but these filamentous features are lost in the CAP-treated cells. The cytoskeleton shrinks and aggregates around the nucleus after CAP treatment (Figure 4d,e). The clear staining of the nucleus suggests that DNA may not suffer noticeable damage immediately after CAP treatment.

The evolution of the treated cells was further investigated on a longer timescale. During this longer observation period, a gradual loss of DNA in the nucleus was seen. The rest of the cell appears to maintain its fixed state, as seen in Figure 2d,e without any further changes during the long period. The bubbles cannot be seen on the cells 2 h after CAP treatment (Figure 5a), which is consistent with the results seen with phase-contrast imaging shown in Figures 2 and 3b. The nucleus of treated cells does expand when compared to the control during the initial 2 h (Figure 5b). However, at the 2 h time mark, the nucleus appears to reach a maximum size and experiences a slight decrease in size after that. The blue DNA staining in the nucleus is seen 1 day after treatment (Figure 5c,d); however, it becomes very weak 2 days after treatment. There is no obvious blue staining of DNA in the nucleus on the third day after CAP treatment, suggesting a total loss of DNA in the nucleus at that time point. The green microtubule staining also gradually weakens by the second day after treatment. Five days after physical CAP treatment, the final appearance of B16F10 cells resembles an empty, circular shell composed of microtubules and other potential cytoskeletal and related cytosolic components not stained in this study (Figure 5d). This matches well with the basic feature of the fixed cells seen in Figure 2d,e. After the loss of all DNA, the cells were determined to be dead and by the sixth day after CAP treatment, we were unable to find any remnants of the cells or any evidence of green microtubule staining. These cell death features are vastly different from the typical apoptotic cell death features observed in previous studies and have not been previously reported in studies of the effect of CAP treatment on cells.

https://dx.doi.org/10.1021/acsami.0c06500
ACS Appl. Mater. Interfaces XXXX, XXX, XXX−XXX

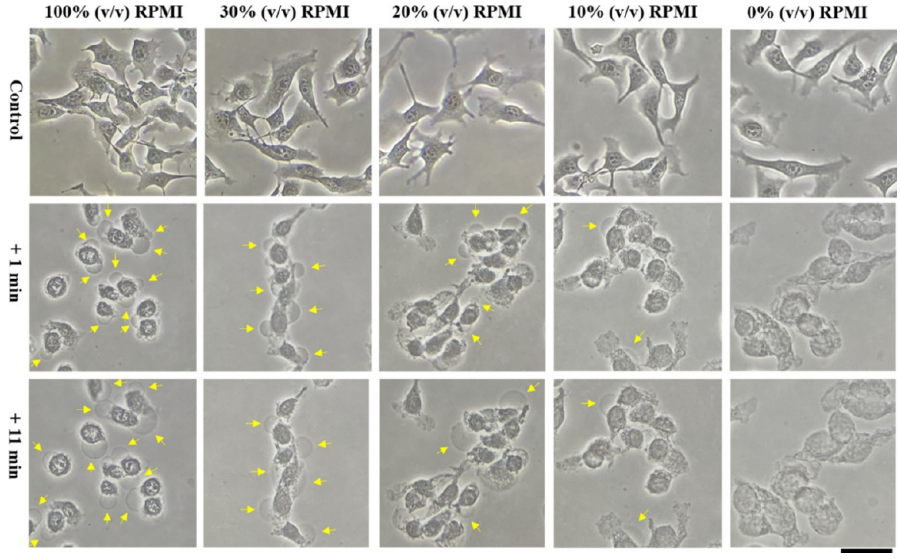

Figure 6. Hypotonic solutions can inhibit the bubbling of the physically treated melanoma cells. The volume ratios % (v/v) of RPMI in the solutions were 100, 30, 20, 10, and 0%. + *x* min means that the photo was taken at *x* min after the CAP treatment. Because the initial bubbles were not clear, only the bubbles after 11 min of growth were marked by yellow arrows. The scale bar was 50 μm (black). Experimental conditions: 10 mL of cell solution was cultured in a 100 mm dish with a density of 7.5×10^4 cells/mL for 1 day before the treatment. In each case, 3 min of CAP treatment was performed on the bottom of an inverted dish. After that, the cells were immediately (<30 s) immersed in the 10 mL of RPMI-1640/Milli-Q water mixed solutions. The photos of control and the experimental group were taken at different places on the dish. The photos of the experimental group were taken in situ. The photo of the CAP jet in the treatment is shown in Figure S6.

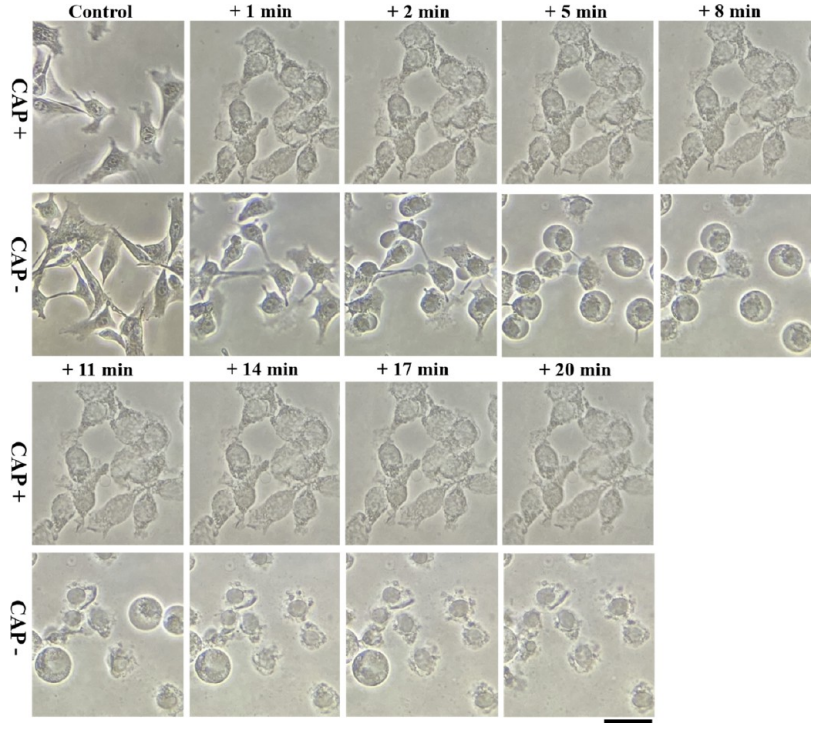

Figure 7. Physically treated melanoma cells are resistant to the osmotic pressure in water. In contrast, the melanoma cells without experiencing the treatment would experience typical cellular responses in the hypotonic solution, a gradual swelling, and final cytolysis. + *x* min means that the photo was taken at *x* min after cells were immersed in Milli-Q water. "CAP +" and "CAP −" represented the cells that experienced or did not experience the CAP treatment, respectively. The scale bar was 50 μm (black). Experimental conditions: 10 mL of cell solution was cultured in a 100 mm dish with a density of 7.5×10^4 cells/mL for 1 day before the treatment. A 3 min of physically based CAP treatment was performed on the bottom of an inverted dish. After that, the cells were immediately (<30 s) immersed in 10 mL of Milli-Q water followed by imaging. The melanoma cells without experiencing the CAP treatment were also immersed in Milli-Q water followed by imaging. The photos of control and the experimental group were taken at different places on the dish. The photos of the experimental group were taken in situ.

The bubbling may be due to changes in osmotic pressure intracellularly. According to the common understanding of bubbling on the cell membrane, the positive intracellular osmotic pressure across the cell membrane should play an

https://dx.doi.org/10.1021/acsami.0c06500
ACS Appl. Mater. Interfaces XXXX, XXX, XXX−XXX

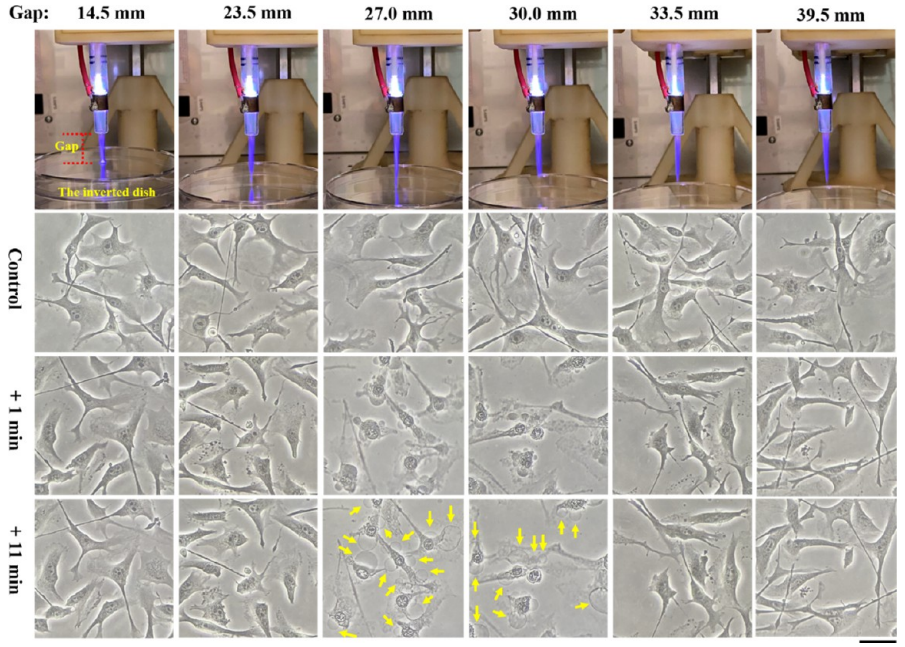

Figure 8. Bubbling only occurs when the CAP source and the bottom surface of an inverted dish has a moderate gap. Neither too small nor too long gap will trigger the bubbling. Experimental conditions: 10 mL of cell solution was cultured in a 100 mm dish with a density of 7.5×10^4 cells/mL for 1 day before the treatment. The 100 mm dish was inverted during the treatment. The gap varied from 14.5 to 39.5 mm. The flow rate was 1.53 lpm for all cases. After the treatment, the cells were immediately (<30 s) immersed in 10 mL of RPMI for microscopic imaging. The photos of control and the experimental group were taken at different places on the dish. The photos of the experimental group were taken in situ. + x min means that the photo was taken at x min after the CAP treatment. Because the initial bubbles were not clear, only the bubbles after 11 min of growth were marked by yellow arrows. The scale bar was 50 μm (black).

important role in regulating the bubbling effect. Such a change in osmotic pressure is mainly due to chemical factors such as the presence of a hypertonic or hypotonic solution in the extracellular chemical environment. In our study, physical treatment is not likely to change the extracellular environment. Our findings may be due to the aggregation of the cytoplasm, which creates intracellular pressure that in turn can trigger the release of water or cytosolic solution across the cell membrane. Physical CAP treatment may also inflict physical damage on the cell, resulting in the formation of pores on the cell membrane through which water or cytosolic solution can be released to form the bubbles.

Deionized (DI) water is a hypotonic solution that causes the influx of water into cells and can therefore potentially counteract the intracellular osmotic pressure and inhibit bubbling. According to this rationale, we prepared a series of RPMI/Milli-Q water (DI water) mixed solutions to investigate the bubbling mechanism. After 3 min of physical CAP treatment, B16F10 cells were immediately turned upright and replenished with different RPMI/Milli-Q mixed solutions. As shown in Figure 6, the density of bubbles forming from the treated cells decreases as the volume ratio of Milli-Q water increases. When the treated cells are immersed in 10 mL of Milli-Q water, the bubbling is completely inhibited. Due to the influx of extracellular water into the cells, the CAP-treated cells also expand in the Milli-Q water. In short, the bubbling may be due to the intracellular osmotic pressure resulting from physical CAP treatment; however, the mechanism is still unknown.

Deionized water such as Milli-Q water will exert a large osmotic pressure on the mammalian cells, which normally will cause the cytolysis after the swelling of cells. We further compared the cellular response of the physical CAP-treated B16F10 cells and the untreated B16F10 cells to Milli-Q water. As shown in Figure 7, the untreated B16F10 cells indeed experienced the typical mammalian cells' response to the hypotonic solution. The cells gradually swelled and formed spheres, most of them detached from the substrate after this stage. Nearly all these sphere-shaped cells finally burst and left debris on the substrate. In contrast, the CAP-treated B16F10 cells did not show noticeable change over the whole imaging process. Such a resistance to the osmotic pressure may be related to the changed mechanical property of cells after the physically based treatment. As we mentioned in Figures 2 and 5, the physically triggered cell death involves the "fixed cellular shape" and forms a shell finally, which may involve the change of the cytoskeletal structure. Such a change may enhance the mechanical property of the cellular membrane and make it against the osmotic pressure without causing the collapse of the cellular membrane.

Bubbling Occurs Even There Is an Air Gap between the Jet and the Target. In all of the cases presented above, the CAP jet directly contacts the bottom of the 96-well plates, 12-well plates, 35 mm culture dishes, or 100 mm culture dishes. As emphasized previously, this treatment method does not involve direct contact of CAP with the cells or the cell medium. Here, we demonstrate that the CAP jet does not have to directly touch the back of the culture dish to cause the effects and cell death seen after physical CAP treatment. We investigated the bubbling triggered after physical CAP treatment at different distances of the nozzle of the CAP source to the back surface of the dish. Some of our conditions in this experiment created a gap between the tip of the jet and the back surface of the dish, as seen in Figure 8. The bubbling will not occur if the gap is too small or too large. Even when the CAP jet noticeably contacts the back surface of the dish,

https://dx.doi.org/10.1021/acsami.0c06500
ACS Appl. Mater. Interfaces XXXX, XXX, XXX−XXX

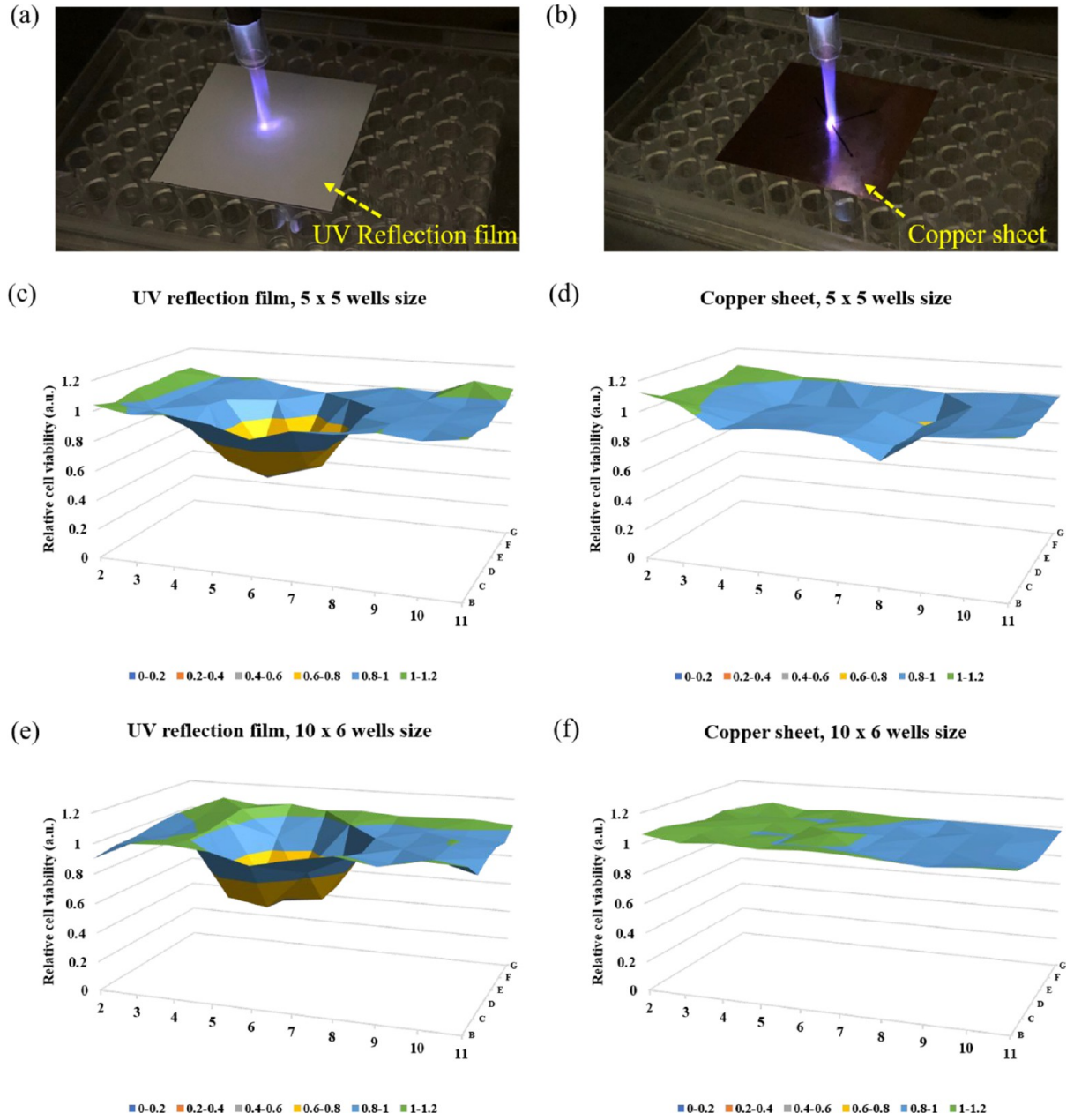

Figure 9. Physically based antimelanoma effects can only be blocked by a copper sheet rather than by a UV reflection film. (a, b) Photos of the physically based CAP treatments on the bottom of 96-well plates covered by the UV reflection film and copper sheet are shown in panels a and b, respectively. Here, we just used the UV reflection film or the copper sheet with a size of 5 × 5 wells as an example. (c–f) Corresponding 2D cell viability is shown in panels c–f. The original data are shown in Figure S10. The treatment was 8 min. The initial cell density was 6×10^4 cells/mL. The cancer cells were cultured 1 day before the final MTT assay. The gap between the nozzle and the bottom surface was 25 mm. The treatment has been independently repeated for four times.

the physical effect will not cause a cellular change. A large distance between the CAP jet and the back surface of the plate of the dish will also not cause the physical effects seen previously. A gap with a distance between 27.0 mm, where the CAP jet is slightly touching the back surface, and 30.0 mm, where there is a small air gap between the tip of jet and the surface, will also trigger bubbling. In the case of a gap of 30.0 mm, the distance between the tip of the jet and back surface is established at 8.2 mm in the image. The corresponding distances for cases of a gap of 33.5 mm and a gap of 39.5 mm are 8.3 and 9.5 mm, respectively. Therefore, there is a significant change in the physical effect on B16F10 cells when the distance between the tip of the jet and the back surface is larger than 8.2 mm.

Physical Factors to Cause Cell Death. To understand the specific role of individual physical factors, we began by analyzing the temperature component of the CAP. We first measured the temperature of the bottom of a 35 mm glass-bottom dish after 2 min of CAP treatment. The maximum temperature of the CAP-treated area was 38.5 ± 0.4 °C (Figure S7). To investigate this heating effect, B16F10 cells in a 35 mm glass-bottom dish were partially immersed in a water bath for 2 min so that the bottom of the dish was immersed in water with a temperature of 41–43 °C. The experimental protocols are illustrated in Figure S8. To simulate physical

https://dx.doi.org/10.1021/acsami.0c06500
ACS Appl. Mater. Interfaces XXXX, XXX, XXX−XXX

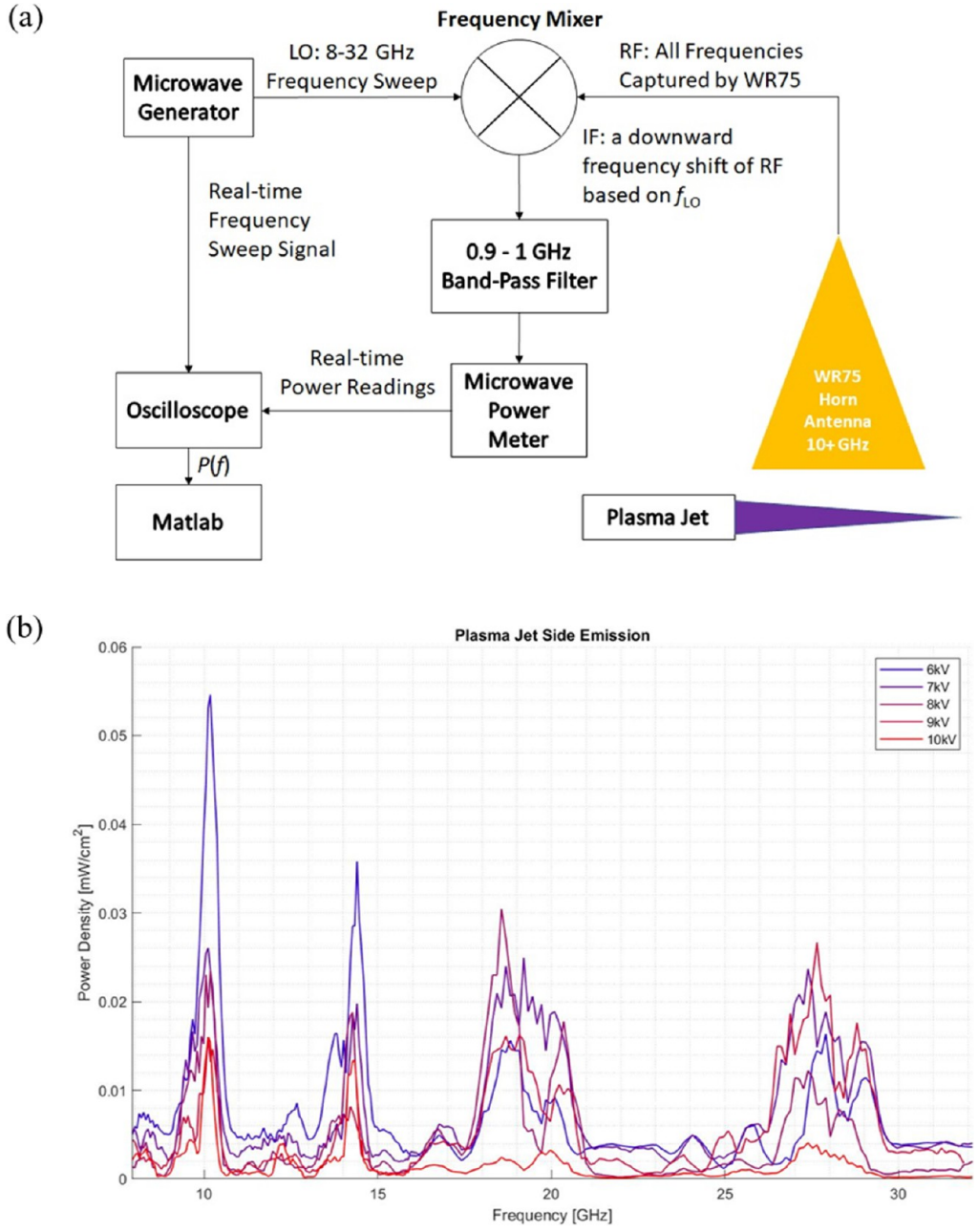

Figure 10. EM emission of the CAP jet under different discharge voltages (pk-pk). (a) Heterodyne setup for RF power spectrum measurement. (b) RF spectra of the CAP jet over 8−32 GHz.

CAP treatment, the media were removed before the heating experiment. This water bath experiment did not cause any change in cell morphology when compared to the control group. In contrast, 2 min of physical CAP treatment caused the drastic cell morphology changes and cell death of B16F10 cells described earlier (Figure S8). Therefore, the heating effect alone does not cause the anticancer effect seen after the physical CAP treatment.

We further investigated the roles of UV radiation and EM waves emitted during physical CAP treatment. A UV reflection film was used to block the UV radiation generated by the CAP jet. The UV reflection film was purchased from VWR (adhesive white light-reflecting films, 89087-696). The characterization of the UV reflection film is shown in Figure S9. The UV reflection film has an excellent attenuation of the UV between 191 and 400 nm. The film was attached to the bottom surface of 96-well plates, centered on well 6D (Figure 9a). The film was removed after treatment. Two sizes of the UV film were used (5 × 5 wells and 10 × 6 wells), which covered 5 × 5 wells and 10 × 6 wells on the bottom of the 96-well plate, respectively. Similarly, to investigate the EM effect, we used a copper sheet as an EM wave blocker with two sizes (5 × 5 wells and 10 × 6 wells). The copper sheets were purchased from McMaster-Carr (9709k704). The copper sheet was set between the CAP jet and the bottom of the 96-well plate during the treatment (Figure 9b). The sheet was also centered at the well 6D. It is found that 8 min of CAP treatment still causes strong growth inhibition even in the presence of a UV reflection film, regardless of size (Figure 9c,e). Unlike the UV reflection films, the 5 × 5 well size copper

https://dx.doi.org/10.1021/acsami.0c06500
ACS Appl. Mater. Interfaces XXXX, XXX, XXX−XXX

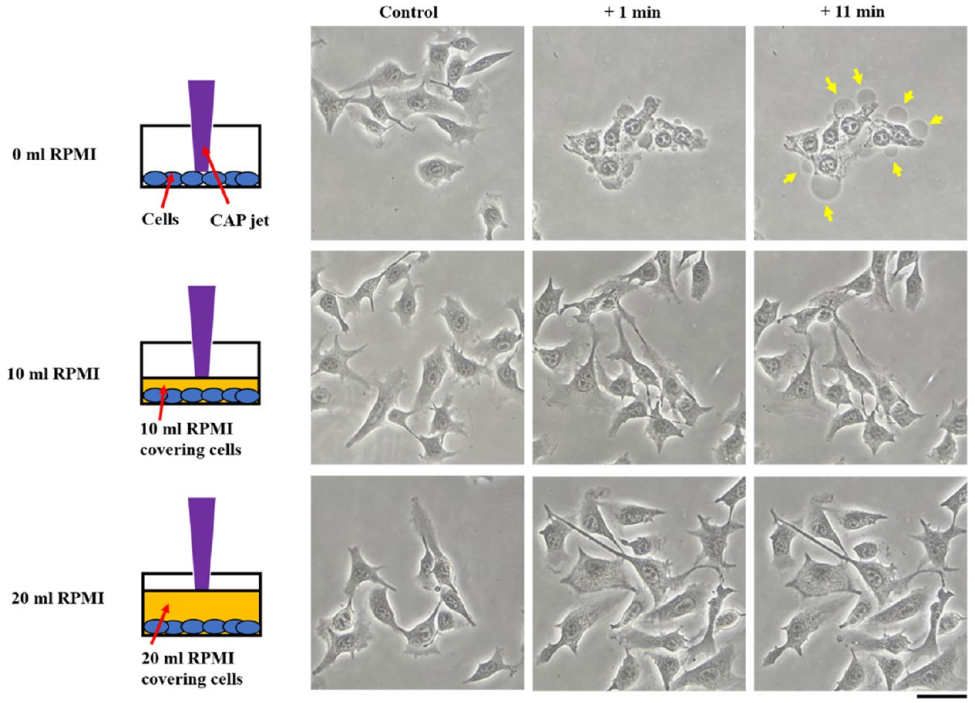

Figure 11. Layer of the medium can completely block the physically triggered bubbling. Different from the above cases, the CAP treatment here was performed by directly touching the melanoma cells without or with a layer of the medium with different volumes (10 and 20 mL). After the treatment, the cells were immediately (<30 s) immersed in 10 mL of RPMI for microscopic imaging. The photos of control and the experimental group were taken at different places on the dish. The photos of the experimental group were taken in situ. Because the initial bubbles were not clear, only the bubbles after 11 min of growth were marked by yellow arrows. The scale bar was 50 μm (black). + x min means that the photo was taken at x min after the CAP treatment. Experimental conditions: 10 mL of cell solution was cultured in a 100 mm dish with a density of 7.5×10^4 cells/mL for 1 day before the treatment. The flow rate was 1.53 lpm. The gap between the nozzle and the cells was 19 mm.

sheet nearly eliminates the typical 2D cell viability map seen after treatment (Figure 9d), and the larger 10 × 6 well sheet is able to completely counteract the antimelanoma effect (Figure 9f). This data led us to theorize that the EM waves produced by the CAP jet play an important role in causing the antimelanoma effect seen after physical CAP treatment. This conclusion also supports the phenomenon that bubbling will still exist even if the tip of the CAP jet does not directly touch the back surface of the dish (Figure 8).

Although the chemical components of CAP have been extensively studied over the past decade using the optical emission spectrum (OES) and laser-induced fluorescence, the EM wave generation in the radio frequency (RF) range by CAP is unknown. A heterodyne setup was designed to measure the RF emission from the CAP jet (Figure 10). The description of the RF spectrum measurement is illustrated in Methods and Materials. Figure 10b shows the RF emission spectra of the CAP jet under different discharge voltages (pk-pk). The spectrum has four peaks. For the peaks at around 10 and 14.5 GHz, a higher discharge voltage leads to a lower power density. However, for the two peaks at a higher frequency, increasing the discharge voltage may first increase the power and subsequently decrease it. The power density reaches its maximum value when the discharge voltage is around 8 kV (pk-pk). In addition, for some power density peaks, the frequency shifts can also be observed on the spectrum. This is the first demonstration of the RF range EM waves generated by the CAP jet. This measurement supports the conclusion that the EM waves generated by CAP can trigger the physically based cell death.

Key Role of the Medium in the Direct CAP Treatment *In Vitro*. Over the past decade, the main focus in plasma medicine has been on the dominant role of reactive species in the CAP−cell interaction, particularly the cytotoxicity of CAP on mammalian cells such as cancer cells.[22] In this study, we demonstrated that an even stronger anticancer effect can be achieved by the physical factors of CAP. We theorize that these effects were seen because nearly all prior *in vitro* studies had a medium layer covering the cells. We believe that EM waves generated by CAP treatment can be absorbed by bulk aqueous solution; therefore, only the chemical effect of CAP was seen in the *in vitro* studies done previously. The biological effects seen after physical CAP treatment should be observed when treatment is done on the back surface of the dish or on the cell directly without the medium coverage.

To test this hypothesis, we performed a direct CAP treatment on cells without the coverage by the medium as well as a treatment on cells with varying volumes of medium coverage (Figure 11). It is found that direct CAP treatment on exposed B16F10 cells (no medium coverage) resulted in shrinkage of the cytoplasm and bubbling from the cell membrane. The 10 mL and 20 mL of the medium layer in a 100 mm dish had a thickness of 1.3 and 2.6 mm, respectively. In both cases, 10 and 20 mL, the physical effects of CAP were not observed. In other words, just a medium layer (1.3 mm) can block the EM waves generated from CAP *in vitro*. This may be the reason that all previous studies could not find evidence of a physical effect if following standard *in vitro* culture conditions. Even a similar cell death has been observed before, it is difficult to investigate the underlying mechanism

https://dx.doi.org/10.1021/acsami.0c06500
ACS Appl. Mater. Interfaces XXXX, XXX, XXX−XXX

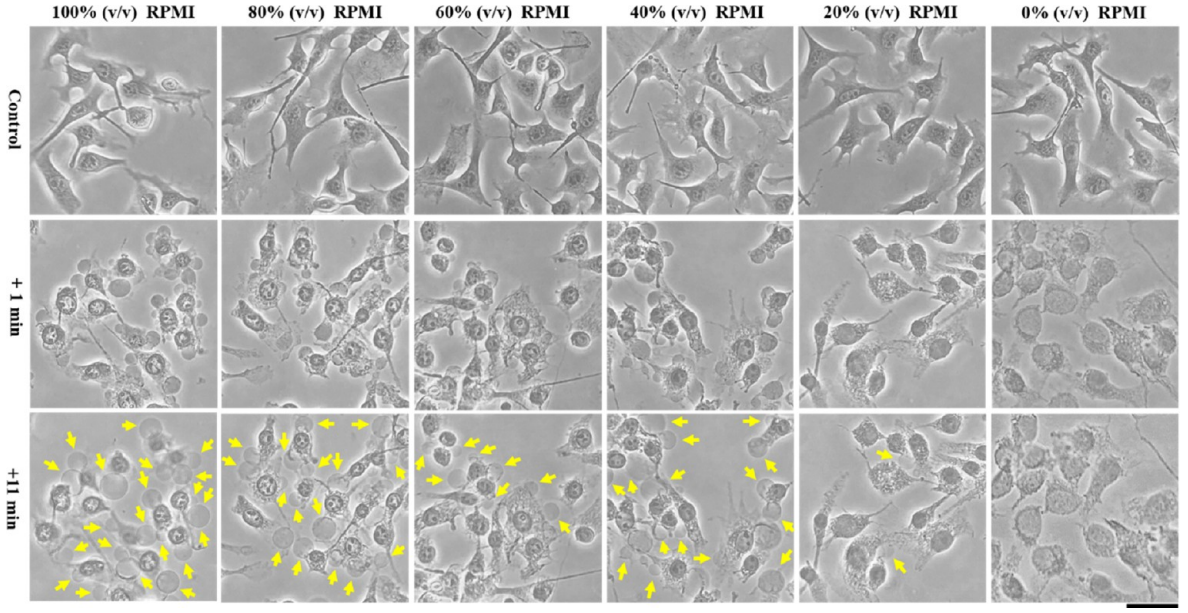

Figure 12. Hypotonic solution can inhibit the bubbling on the direct CAP treatment on melanoma cells without the coverage of a medium layer. A 3 min of CAP treatment was performed on the cells without the coverage of a medium layer. The treated cells were immediately (<30 s) immersed in 10 mL of RPMI/Milli-Q water mixed solutions. The volume ratios % (v/v) of RPMI in the solutions were 100, 80, 60, 40, 20, and 0%. The photos of control and the experimental group were taken at different places on the dish. The photos of the experimental group were taken in situ. + *x* min means that the photo was taken at *x* min after the CAP treatment. Because the initial bubbles were not clear, only the bubbles after 11 min of growth were marked by yellow arrows. The scale bar was 50 μm (black). Experimental conditions: the seeding cell density was 7.5×10^4 cells/mL. Cell solution (10 mL) was cultured in a 100 mm dish for 1 day before the treatment. The flow rate was 1.53 lpm. The gap between the nozzle and the cells was 19 mm.

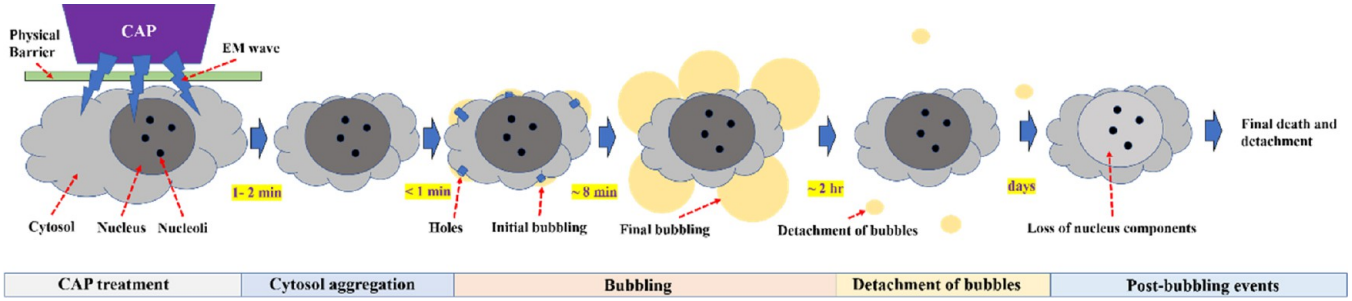

Figure 13. Schematic illustration of the whole process of physically triggered cell death. Cell death has main four stages: cytosol aggregation, bubbling, detachment of bubbles, and post-bubbling events. The first two stages are quick cellular response, totally lasting around 10 min. The detachment of bubbles may last more than 1−2 h. In contrast, the post-bubbling events may last days. The bubbling may be a process that the cells drastically lose it water components. The main cytosol shape will not change after the first stage, which gives the cells an appearance as having been fixed after the treatment. Such a "fix shape" will be kept over days until the final cell death or detachment.

due to the complex nature of the direct interaction between the CAP jet and the cells.

We further investigated whether the bubbling could be inhibited by exposure to various hypotonic solutions after direct CAP treatment on the cells without a medium coverage. Similar to the trend shown in Figure 6, we found that an increase in the volume ratio of Milli-Q water gradually inhibited bubble production, and the bubble growth is completely inhibited in solely Milli-Q solution (Figure 12). These results indicate that the physical effect of the CAP jet will impact cancer cells in the same way regardless of treatment from the back of a plate or dish or direct treatment of cells without the medium coverage. We conclude that medium blocks physically based cytotoxicity; therefore, only the chemical factors will play an anticancer role in this case as was found in prior studies.

DISCUSSION

This study is unique because it focused on the physical factors and physical effect of CAP rather than on the previously studied chemical effect and CAP-originated reactive species. This physical factor-based CAP treatment may clarify many of the puzzles in plasma medicine, which cannot be explained by the reactive species-based perspective. As illustrated in this study, reactive species are not necessary to achieve a strong anticancer effect after CAP treatment. Additionally, the bulk aqueous environment is not a prerequisite for CAP treatment to be effective. B16F10 cells are much more sensitive to the physical factor in CAP than the chemical factors in CAP. In our experiments, we found that physical CAP treatment could affect a larger area of cells compared to chemical CAP treatment. Thus, we provide a solution to overcome the natural

https://dx.doi.org/10.1021/acsami.0c06500
ACS Appl. Mater. Interfaces XXXX, XXX, XXX−XXX

limitation of traditional CAP treatment based on the cellular sensitivity to the cytotoxicity of reactive species.

Physical CAP treatment causes a new type of cell death characterized by the bulk leakage of water out of the cell and cytosol aggregation (Figure 13). These changes are seen just a couple of minutes after treatment, a much faster process than the typical apoptosis pathway. The bubbling may be due to the formation of holes on the cytoplasmic membrane, which has not been confirmed, and can be speculated from the observation of growth of new bubbles (Videos S1 and S2). The long-term changes seen in the cells after physical CAP treatment are also unique. The cells gradually lose DNA from the nucleus over the course of 1−2 days after treatment. The aggregated cytoskeleton stays intact for 3−5 days after treatment, which may finally form an empty shell. We called such an empty shell as the fixed cells after the treatment. These features are very different from apoptotic features and have never been reported before.

Physical CAP treatment builds a connection between *in vitro* and *in vivo* experiments. Previous studies have concluded that apoptosis is the main form of cell death following chemical CAP treatment. The apoptosis will not trigger an immune or inflammation response *in vitro*; however, several *in vivo* animal studies found a noticeable immune response during the CAP treatment.[23−26] The conventional reactive species-based plasma medicine perspective cannot explain this immunologic dilemma. However, this newly discovered cell death, clear necrosis involving bulk leakage of water or cellular solutions will likely trigger an immune response *in vivo* if the same changes that occur *in vitro* are seen during *in vivo* studies.

The transdermal diffusion of reactive species may be necessary for the explanation of the *in vivo* anticancer effect of the reactive species-based CAP treatment.[27,28] However, there is no obvious evidence so far indicating the existence of a strong transdermal diffusion of ROS, particularly H_2O_2, an important anticancer reactive species *in vitro*.[29] As demonstrated in this study, the physical effect can penetrate a dielectric material with a thickness of 1.3 mm, which is close to the thickness of human skin. Although the material property of the cell culture dish or plates is different from human skin, we propose that the same physical effect may also exist when CAP just treat on the skin without directly contacting the tumor. Our observations suggest that it may not be necessary to assume that transdermal diffusion of reactive species exists when CAP treatment is performed above animal skin.

The underlying mechanism of the physical antimelanoma effect is still unknown. Take red blood cells as an example, when they are in the hypotonic solution, they will swell and even finally burst. In contrast, when the red blood cells are in the hypertonic solution, they will experience shrinkage and lose water. Based on these common senses, the physically triggered cell death indeed looks like when the cells are in a hypertonic solution. However, the bubbling occurs when the physically triggered cells are immersed in the medium, an isotonic solution. According to the common understanding of osmotic pressure, there should either have more water components in the treated cells or have less solute in the intracellular solutions. So far, there is no experimental evidence to support both two speculations. Based on the microscopic observation, the physical factors trigger the aggregation first, which may then trigger the bubbling by forming an intracellular osmotic pressure. Also, the holes may form on the cellular membrane to facilitate the bubbling based on Videos S1 and S2.

The connection between the EM wave and the cytosol aggregation is also unknown. The reason to cause the fixed shape of cells after the treatment is also unknown. At this time, we just discuss the possible biological effect of the EM wave based on previous references. As shown in Figure 8, the bulk CAP can detach from the bottom of the dish with an air gap around 8 mm. This feature supports the propagation of the EM wave from the bulk CAP to the cellular target. In the past, the interaction of mm-wavelength EM with living cells was considered extensively. The importance of this interaction stems from the fact that biological species on earth are not very well accustomed to this type of interaction. This idea was proposed by Devyatkov et al. who believed that living organisms on earth are not well adapted to this type of radiation because under natural conditions it is practically absent due to strong absorption by the earth's atmosphere.[30] This is due to the fact that mm-wavelength is absorbed by water molecules in the rotational mode. Several important discoveries were reported such as the dependence of EM action on cells on frequency when various microorganisms are irradiated by mm-waves.[31] In addition, *in vivo* studies were performed to evaluate the effect of mm-wave on tumors and the growth of cells damaged by the ionizing radiation.[32] To that end, the isolated cells damaged by ionizing radiation were consequently irradiated with EM waves at frequencies of 54−76 GHz and power density of 10^{-16}−10^{-14} W/cm^2 for 7 min.[32] The effect of mm-waves at frequencies of 35.9−55.1 GHz on the growth of implanted tumors (such as carcinomas) in mice and rats has been studied.[32] The power was applied via acupuncture points. These experiments showed that mm-waves at nonthermal intensities act to normalize the growth of cells damaged by the ionizing radiation, and in their action on biologically active zones in animals, they have an immunomodulating effect. The CAP jet generates EM waves having a similar frequency as shown in Figure 10, which is likely causing the observed cell death.

CONCLUSIONS

The physical factors of CAP treatment show strong growth inhibition on B16F10 cells, a typical melanoma cell line. Compared to traditional chemical CAP treatment, physical CAP treatment shows a much stronger growth inhibition on melanoma cells *in vitro*. The electromagnetic waves emitted from the CAP jet could cause cell death through a physical barrier (∼1 mm) without contacting the cells as well as through direct contact with cells not covered by the medium. Cell death following physical CAP treatment is characterized by rapid bulk leakage of water through the cell membrane accompanied by the cytosol aggregation. The bubbling seen on the cell membrane is a typical feature of necrotic cell death. The bubbling may be triggered by the physically triggered osmotic pressure, which can be inhibited in the hypotonic solutions. This study builds the foundation for using CAP as a physically based noninvasive anticancer therapy and possibly applying CAP treatment in various other branches of medicine.

METHODS AND MATERIALS

CAP Jet. The CAP jet was designed and assembled at Keidar's laboratory at the George Washington University. The detailed introduction of this device, particularly the optical emission spectrum (OES) of bulk CAP, the discharge voltage, and the discharge current of the CAP jet device have been demonstrated in our previous publications.[21,33,34] Briefly, the CAP jet was formed through the

https://dx.doi.org/10.1021/acsami.0c06500
ACS Appl. Mater. Interfaces XXXX, XXX, XXX−XXX

discharge (3.15 kV, peak value) between a copper ring grounded cathode and a central stainless anode. The ionized gas was flowed out by helium guided in a glass tube with a diameter of 4.5 mm. The maximum tip temperature of the CAP jet during the treatment was around 40 °C.

Cell Culture. B16F10 cells were donated by Prof. Eduardo Sotomayor at the George Washington University. The cell culture medium was composed of RPMI-1640 (ATCC 30-2001) supplemented with 10% fetal bovine serum (Atlanta Biologicals, S11150) and 1% (v/v) penicillin and streptomycin solution (Life Technologies, 15140122). For the CAP treatment performed on a 96-well plate, B16F10 cells were seeded (100 μL/well) in a 96-well plate with a density of 6×10^4 cells/mL. For the CAP treatment performed on a 12-well plate, B16F10 cells were seeded (1 mL/well) in a 12-well plate with a density of 5×10^4 cells/mL. All cells were cultured 24 h under the standard culture condition (a humidified, 37 °C, 5% CO_2 environment) before the experiments.

Chemically Based and Physically Based CAP Treatments. For the cases using a 96-well plate, to perform the chemically based CAP treatment, the medium used in the previous culture for 24 h was removed first. Then, 100 μL/well of fresh RMPI-1640 medium was added to cover all 10×6 wells in the middle of the 96-well plate. The chemically based CAP treatment (1, 4, or 8 min) was performed after this step. After the treatment, the cancer cells were cultured for 2 days before the cell viability assay. To perform the physical CAP treatment, the medium used in the previous culture for 24 h was also removed first. Due to the surface tension and the adhesion of water, there was a thin water layer in each well, particularly at the junction between the wall and the bottom in a well. Although there was no bulk medium left to cover the cells during the treatment, the cell viability of cancer cells did not decrease (Figure S2). After the treatment, 100 μL/well of RMPI-1640 was added to culture the cells in the middle 10×6 wells. The treated cells were cultured 2 days before the cell viability assay.

For the cases using a 12-well plate, the general strategy to perform the chemical and the physical treatments was unchanged. A single chemical treatment was performed in a single well with a 1 mL of RPMI-1640 medium. A single physical treatment was performed on the back of a single well without medium coverage. After the treatment, 1 mL/well of RMPI-1640 was added to culture the cells for 3 days before the cell viability assay. The wells on the 12-well plate were much larger than those of 96-well plates. The treatment on a single well only affected the treated well. Thus, for the 12-well plate case, we just used the traditional single well's cell viability to describe the physically based antimelanoma effect.

Cell Viability Assay. The cell viability assay was performed using the MTT assay according to the protocols provided by the manufacturer (Sigma-Aldrich, M2128). The absorbance at 570 nm was read using an H1 microplate reader (Hybrid Technology). For the 96-well plate, because the whole middle 10×6 wells on each plate were used to quantify the anticancer effect in each case, we used 2D cell viability map to quantify the antimelanoma effect. This is a novel strategy to show the cell viability, and the detailed protocols are illustrated in Figure S1. The 2D cell viability map shows all the cell viability data of 10×6 wells simultaneously. For the 12-well plate, the relative cell viability was obtained by the division between the experimental group and the mean value of the control group. As shown in Figure 2b,c, the mean value represents the average of six wells as the control group, which includes the three wells in the first and the last column from the left to the right.

Live-Cell Fluorescence Imaging. We seeded 600 μL of B16F10 cells (3×10^3 cells/mL) on the 35 mm confocal observation glass-bottom dish and cultured 2 days before the treatment. After a proper adherence of cells, the morphological changes in the live melanoma cells were assessed by staining microtubules (BioTracker 488 Green microtubule cytoskeleton dye, Sigma-Aldrich) and DNA (Hoechst 33342 staining dye solution, Thermo Fisher Scientific). B16F10 cells were stained with both dyes after an overnight culture incubation. The dye working concentration for the microtubule staining was 1 μL in 1 mL (0.1%), and the DNA staining was 1 μg/mL in RPMI-1640 media. The cells were incubated for 15 min inside the CO_2 incubator before the CAP treatment.

RF Spectrum Measurement. The RF emission containing multiple frequency components was collected using a WR-75 horn antenna, which works for 10+ GHz microwave. The frequency mixer shifted the signal to a lower frequency range based on the local oscillator (LO) signal, which was provided by a microwave generator. Since the LO was a frequency sweeping signal from 8 to 32 GHz, the resulting output intermediate frequency (IF) signal was the same spectrum of RF but keeping a downward frequency shifting. The IF then passed through a 0.9−1 GHz band-pass filter. The microwave power meter thus integrated the total power through the filter window. Since the IF kept shifting, a full picture of emission power was obtained. The microwave power meter provided the power as a function of time, while the microwave generator reported the frequency shift as a function of time. A power spectrum was finally obtained.

■ ASSOCIATED CONTENT

Supporting Information

The Supporting Information is available free of charge at https://pubs.acs.org/doi/10.1021/acsami.0c06500.

Figure S1, generation of 2D cell viability map; Figure S2, placing the inverted 96-well plate for 10 min without the CAP treatment did not change cell viability; Figure S3, original data of Figure 1; Figure S4, some typical bubbles on the CAP-treated B16F10 cells; Figure S5, continuous observation of the bubbling; Figure S6, photo for the physically based CAP treatment in Figure 6; Figure S7, measured temperature on the bottom of the 35 mm dish after 2 min of CAP treatment; Figure S8, heating experiment in the water bath (41−43 °C) will not cause the same cell death due to CAP treatment (2 min); Figure S9, characterization of the UV blockage effect of the UV reflection film from 190 to 400 nm using the optical emission spectrum (OES); and Figure S10, original data of Figure 9 (PDF)

Video S1, growth of bubbles from a single point on the cellular membrane. The real-time length of this video was 15 min 18 s (MP4)

Video S2, growth of bubbles from another single point on the cellular membrane. The real-time length of this video was 15 min 18 s (MP4)

■ AUTHOR INFORMATION

Corresponding Authors

Dayun Yan − *Department of Mechanical and Aerospace Engineering, The George Washington University, Washington, D.C. 20052, United States;* orcid.org/0000-0002-9801-021X; Email: ydy2012@gwmail.gwu.edu

Michael Keidar − *Department of Mechanical and Aerospace Engineering, The George Washington University, Washington, D.C. 20052, United States*; Email: keidar@gwu.edu

Authors

Qihui Wang − *Department of Mechanical and Aerospace Engineering, The George Washington University, Washington, D.C. 20052, United States*

Manish Adhikari − *Department of Mechanical and Aerospace Engineering, The George Washington University, Washington, D.C. 20052, United States*

Alisa Malyavko − *School of Medicine and Health Sciences, The George Washington University, Washington, D.C. 20052, United States*

https://dx.doi.org/10.1021/acsami.0c06500
ACS Appl. Mater. Interfaces XXXX, XXX, XXX−XXX

Li Lin − *Department of Mechanical and Aerospace Engineering, The George Washington University, Washington, D.C. 20052, United States*

Denis B. Zolotukhin − *Department of Mechanical and Aerospace Engineering, The George Washington University, Washington, D.C. 20052, United States;* orcid.org/0000-0002-5206-9486

Xiaoliang Yao − *Department of Mechanical and Aerospace Engineering, The George Washington University, Washington, D.C. 20052, United States*

Megan Kirschner − *Department of Mechanical and Aerospace Engineering, The George Washington University, Washington, D.C. 20052, United States*

Jonathan H. Sherman − *Neurological Surgery, The George Washington University, Washington, D.C. 20037, United States*

Complete contact information is available at: https://pubs.acs.org/10.1021/acsami.0c06500

Author Contributions

‖D.Y., Q.W., and M.A. contributed equally to this manuscript.

Notes

The authors declare no competing financial interest.

■ ACKNOWLEDGMENTS

This work was supported by the National Science Foundation, grant 1747760. The authors would like to thank for the instructive training and warm help from Prof. Anastas Popratiloff at the Nanofabrication and Imaging Center of George Washington University.

■ REFERENCES

(1) Miller, A. J. Mihm, M. C. Melanoma. *N. Engl. J. Med.* **2006**, *355*, 51−65.

(2) Thompson, J. F.; Scolyer, R. A.; Kefford, R. F. Cutaneous Melanoma. *Lancet.* **2005**, *365*, 687−701.

(3) Linares, M. A.; Zakaria, A.; Nizran, P. Skin Cancer. *Primary care Clin. Off. Pract.* **2015**, *42*, 645−659.

(4) Soengas, M. S.; Lowe, S. W. Apoptosis and Melanoma Chemoresistance. *Oncogene* **2003**, *22*, 3138−3151.

(5) Peach, A. H. S. Cutaneous Melanoma. *Surgery.* **2006**, *24*, 21−26.

(6) Ivanov, V. N.; Bhoumik, A.; Ronai, Z. E. Death Receptors and Melanoma Resistance to Apoptosis Oncogene. 2003, *22* (20), 3152−3161.

(7) Fridman, A.; Chirokov, A.; Gutsol, A. Non-thermal Atmospheric Pressure Discharges. *J. Phys. D: Appl. Phys.* **2005**, *38*, R1−R24.

(8) Laroussi, M.; Akan, T. Arc-free Atmospheric Pressure Cold Plasma Jets: A Review. *Plasma Processes Polym.* **2007**, *4*, 777−788.

(9) Graves, D. B. Reactive Species from Cold Atmospheric Plasma: Implications for Cancer Therapy. *Plasma Processes Polym.* **2014**, *11*, 1120−1127.

(10) Keidar, M. Plasma for Cancer Treatment. *Plasma Sources Sci. Technol.* **2015**, *24*, No. 033001.

(11) Keidar, M.; Shashurin, A.; Volotskova, O.; Ann Stepp, M.; Srinivasan, P.; Sandler, A.; Trink, B. Cold Atmospheric Plasma in Cancer Therapy. *Phys. Plasmas* **2013**, *20*, No. 057101.

(12) Yan, D.; Sherman, J. H.; Keidar, M. Cold Atmospheric Plasma, a Novel Promising Anti-cancer Treatment Modality. *Oncotarget* **2017**, *8*, 15977−15995.

(13) Kim, S. J.; Chung, T. H.; Bae, S. H.; Leem, S. H. Induction of Apoptosis in Human Breast Cancer Cells by A Pulsed Atmospheric Pressure Plasma Jet. *Appl. Phys. Lett.* **2010**, *97*, No. 023702.

(14) Ahn, H. J.; Kim, K. I.; Kim, G.; Moon, E.; Yang, S. S.; Lee, J.-S. Atmospheric-Pressure Plasma Jet Induces Apoptosis Involving Mitochondria via Generation of Free Radicals. *PLoS One* **2011**, *6*, e28154.

(15) Panngom, K.; Baik, K. Y.; Nam, M. K.; Han, J. H.; Rhim, H.; Choi, E. H. Preferential Killing of Human Lung Cancer Cell Lines with Mitochondrial Dysfunction by Nonthermal Dielectric Barrier Discharge Plasma. *Cell Death Dis.* **2013**, *4*, No. e642.

(16) Ahn, H. J.; Kim, K. I.; Hoan, N. N.; Kim, C. H.; Moon, E.; Choi, K. S.; Yang, S. S.; Lee, J.-S. Targeting Cancer Cells with Reactive Oxygen and Nitrogen Species Generated by Atmospheric-Pressure Air Plasma. *PLoS One* **2014**, *9*, e86173.

(17) Adamovich, I.; Baalrud, S. D.; Bogaerts, A.; Bruggeman, P. J.; Cappelli, M.; Colombo, V.; Czarnetzki, U.; Ebert, U.; Eden, J. G.; Favia, P.; Graves, D. B.; Hamaguchi, S.; Hieftje, G.; Hori, M.; Kaganovich, I. D.; Kortshagen, U.; Kushner, M. J.; Mason, N. J.; Mazouffre, S.; Thagard, S. M.; Metelmann, H. R.; Mizuno, A.; Moreau, E.; Murphy, A. B.; Niemira, B. A.; Oehrlein, G. S.; Petrovic, Z. L.; Pitchford, L. C.; Pu, Y.-K.; Rauf, S.; Sakai, O.; Samukawa, S.; Starikovskaia, S.; Tennyson, J.; Terashima, K.; Turner, M. M.; van de Sandan, M. C. M.; Vardelle, A. The 2017 Plasma Roadmap: Low Temperature Plasma Science and Technology. *J. Phys. D: Appl. Phys.* **2017**, *50*, 323001.

(18) Keidar, M.; Yan, D.; Beilis, I. I.; Trink, B.; Sherman, J. H. Plasmas for Treating Cancer: Opportunities for Adaptive and Self-adaptive Approaches. *Trends Biotechnol.* **2018**, *36*, 586−593.

(19) Keidar, M. A Prospectus on Innovations in the Plasma Treatment of Cancer. *Phys. Plasmas* **2018**, *25*, No. 083504.

(20) Graves, D. B. Lessons from Tesla for Plasma Medicine. *IEEE Trans. Radiat. Plasma Med. Sci.* **2018**, *2*, 594−607.

(21) Yan, D.; Lin, L.; Sherman, J. H.; Canady, J.; Trink, B.; Keidar, M. The Between the Cytotoxicity of Cold Atmospheric Plasma and the Extracellular H2O2-Scavenging RateThe Correlation between the Cytotoxicity of Cold Atmospheric Plasma and the Extracellular H2 O2-scavenging Rate. *IEEE Trans. Radiat. Plasma Med. Sci.* **2018**, *2*, 618−623.

(22) Graves, D. B. The Emerging Role of Reactive Oxygen and Nitrogen Species in Redox Biology and Some Implications for Plasma Applications to Medicine and Biology. *J. Phys. D: Appl. Phys.* **2012**, *45*, 263001.

(23) Mizuno, K.; Yonetamari, K.; Shirakawa, Y.; Akiyama, T.; Ono, R. Anti-tumor Immune Response Induced by Nanosecond Pulsed Streamer Discharge in Mice. *J. Phys. D: Appl. Phys.* **2017**, *50*, 12LT01.

(24) Lin, A.; Truong, B.; Patel, S.; Kaushik, N.; Choi, E. H.; Fridman, G.; Fridman, A.; Miller, V. Nanosecond-pulsed DBD Plasma-generated Reactive Oxygen Species Trigger Immunogenic Cell Death in A549 Lung Carcinoma Cells through Intracellular Oxidative Stress. *Int. J. Mol. Sci.* **2017**, *18*, 966.

(25) Lin, A.; Gorbanev, Y.; Cos, P.; Smits, E.; Bogaerts, A. Plasma Elicits Immunogenic Death in Melanoma Cells. *Clin. Plasma Med.* **2018**, *9*, 9.

(26) Lin, A.; Gorbanev, Y.; De Backer, J.; Van Loenhout, J.; Van Boxem, W.; Lemière, F.; Cos, P.; Dewilde, S.; Smits, E.; Bogaerts, A. Non-thermal Plasma as a Unique Delivery System of Short-lived Reactive Oxygen and Nitrogen Species for Immunogenic Cell Death in Melanoma Cells. *Adv. Sci.* **2019**, *6*, 1802062.

(27) Lu, X.; Keidar, M.; Laroussi, M.; Choi, E.; Szili, E. J.; Ostrikov, K. Transcutaneous Plasma Stress: From Soft-matter Models to Living Tissues. *Mater. Sci. Eng. R Reports* **2019**, *138*, 36−59.

(28) Szili, E. J.; Oh, J. S.; Fukuhara, H.; Bhatia, R.; Gaur, N.; Nguyen, C. K.; Hong, S. H.; Ito, S.; Ogawa, K.; Kawada, C.; Shuin, T. Modelling the Helium Plasma Jet Delivery of Reactive Species into a 3D Cancer Tumour. *Plasma Sources Sci. Technol.* **2017**, *27*, No. 014001.

(29) Liu, X.; Gan, L.; Ma, M.; Zhang, S.; Liu, J.; Chen, H.; Liu, D.; Lu, X. A Comparative Study on the Transdermal Penetration Effect of Gaseous and Aqueous Plasma Reactive Species. *J. Phys. D: Appl. Phys.* **2018**, *51*, No. 075401.

(30) Devyatkov, N. D.; Golant, M. B.; Betskiy, O. V. Millimeter Waves and Their Role in the Processes of Life Activities. *Moscow. Radio. Commun* **1991**, *168*.

(31) Smolyanskaya, A. Z.; Gel'vich, E. A.; Golant, M. B.; Makhov, A. M. Resonance Phenomena in the Action of Millimeter Waves on Biological Objects. *Usp. Sovrem. Biol.* **1979**, *87*, 381−392.
(32) Bundyuk, L. S.; Kuz'menko, A. P.; Ryabchenko, N. N.; Litvinov, G. S. Corrective Action of Millimeter Waves on Systems of Various Levels of Hierarchy. *Phys. Alive.* **1994**, *2*, 12−25.
(33) Yan, D.; Lin, L.; Xu, W.; Nourmohammadi, N.; Sherman, J. H.; Keidar, M. Universality of Micromolar-Level Cell-Based Hydrogen Peroxide Generation During Direct Cold Atmospheric Plasma Treatment. *Plasma Med.* **2018**, *8*, 335−343.
(34) Yan, D.; Talbot, A.; Nourmohammadi, N.; Cheng, X.; Canady, J.; Sherman, J.; Keidar, M. Principles of Using Cold Atmospheric Plasma Stimulated Media for Cancer Treatment. *Sci. Rep.* **2015**, *5*, 18339.

https://dx.doi.org/10.1021/acsami.0c06500
ACS Appl. Mater. Interfaces XXXX, XXX, XXX−XXX